DESIGN OF A BAND-PASS FILTER USING STEPPED IMPEDANCE RESONATORS WITH FLOATING CONDUCTORS

M. D. C. Velázquez-Ahumada

Department of Electronics and Electromagnetism
University of Seville
Av. Reina Mercedes s/n, Seville 41012, Spain

J. Martel

Department of Applied Physics 2
University of Seville
Av. Reina Mercedes s/n, Seville 41012, Spain

F. Medina

Department of Electronics and Electromagnetism
University of Seville
Av. Reina Mercedes s/n, Seville 41012, Spain

F. Mesa

Department of Applied Physics 1
University of Seville
Av. Reina Mercedes s/n, Seville 41012, Spain

Abstract—A new type of miniaturized stepped impedance resonator (SIR) for bandpass filter applications is proposed in this paper. The new resonator incorporates a ground plane window with a floating conductor in the backside of the substrate. The ground plane window increase the characteristic impedance of the lines used to implement the inductive region of the quasi-lumped resonator, thus allowing some size reduction. Moreover, the presence of a floating conducting patch printed below the capacitive region of the resonator pushes up the first spurious band of the filter. A meaningful improvement of its out-of-band rejection level is then achieved. The coupling between adjacent resonators is also enhanced thus leading to wider achievable

Corresponding author: F. Medina (medina@us.es).

bandwidths. Some filter designs using the new resonator and other standard resonators are included for comparison purposes.

1. INTRODUCTION

Miniaturization of printed planar microwave filters has been a popular research topic in recent years owing to the growing expansion of wireless and mobile communication systems operating at the lower end of the microwave spectrum. Recent examples of this kind of research can be found in [1–7]. Conventional distributed resonators are too large to be used at low frequencies when miniaturization is a key issue. Thus, these resonators have been progressively replaced by smaller structures. Half-wavelength resonators originally used to implement parallel-coupled line filters [8] were substituted by hairpin resonators such as those reported in [9]. A more compact version of the hairpin resonator is the square open-loop resonator [10], but this resonator still works as a distributed device that yields too large layouts at low frequencies. An additional drawback of distributed resonators is the degradation of the out-of-band rejection level because of the existence of undesired spurious harmonics. This problem can be overcome by using compact quasi-lumped resonators at the price of increasing losses. For instance, the folded hairpin resonator in [11] is much smaller than the conventional hal temairpin or open-loop resonators owing to increased capacitance associated to two closely coupled sections. A similar effect can be attained using the miniaturized open-loop resonators proposed in [12], later modified by other authors [13] and now called folded stepped impedance resonators (folded SIR) [14]. This resonator can be viewed as a high characteristic impedance transmission line loaded with a low impedance coupled line pair. For relatively high values of the capacitance of the wide coupled lines section and for the lowest resonance frequency, the structure behaves as an LC quasi-lumped resonator. In such case, the inductance, L, is provided by the short section of high characteristic impedance microstrip line and the capacitance, C, is associated with the electrically short pair of coupled lines. The quasi-lumped nature of the resonator automatically alleviates the problem associated with the presence of the first spurious transmission band [15]. More sophisticated versions of SIR's have been applied to filter design looking for compactness and wide upper stopband behavior [16].

Recently, a number of compact printed resonators have profited from the patterning of the backside metallization of the substrate [17–20] in order to enhance their performance. These are known as defected
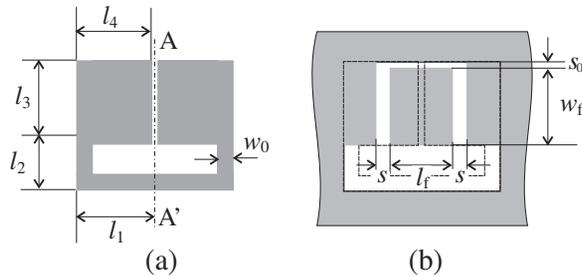
Figure 1. Folded stepped impedance resonator with ground plane window and floating conductor. (a) Top view; (b) bottom view. To clarify the window position in the bottom view, the contour of the upper side resonator has been drawn using dashed lines.

ground structures (DGS). Following that research line, in this paper we propose the new resonator shown in Fig. 1. This resonator, a folded SIR with floating conductor, can be considered a modified version of the resonators proposed in [12, 14]. The ground plane area below the resonator is partially removed, in such a way that a metallic floating rectangular patch remains inside the ground window and below the coupled lines section. The presence of the window increases the characteristic impedance of the single strip section [21–23] thus providing some size reduction. But what is more important in the context of this paper, the floating conductor provides a way to improve the out-of-band rejection level of filters based on this structure. This is a very important issue to avoid intermodulation distortion [24]. Roughly speaking, the first resonance frequency associated with the desired pass band is close to the one of the conventional folded SIR, while the second resonance frequency meaningfully pushed up. This fact allows a better rejection level above the first band. As additional benefits, the ground plane window opens a new coupling mechanism improving the coupling factor between neighbor resonators [25] thus making possible wider bandwidths. In brief, the new resonator allows us to built filters slightly smaller than the ones based on conventional folded SIRs with larger achievable bandwidths and better rejection level above the first pass band.
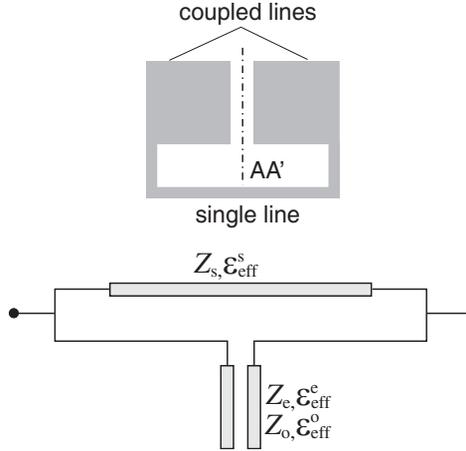
Figure 2. Transmission line circuit model of any folded SIR. The model is valid for conventional folded SIR and approximately accounts for the behavior of the folded SIR with floating conductor.

2. CHARACTERIZATION OF SINGLE RESONATORS

2.1. Transmission Line Circuit Model

Fig. 2 shows a transmission line circuit model that reasonably accounts for the electromagnetic behavior of folded SIR's. For the folded SIR with floating conductor studied in this paper this is just an approximate model because the coupled section involves three conductors plus ground. Three, instead of two, quasi-TEM modes are then involved. However, it has been shown in the past that the even/odd mode theory reasonably applies to this case [26, 27]. The characteristic impedance and the effective dielectric constant of the single transmission line section, providing the inductive contribution, are Z_s and $\varepsilon_{\text{eff}}^s$ respectively. The capacitive part of the resonator can be viewed as a coupled pair of microstrip lines whose electrical parameters are the even (e) and odd (o) mode characteristic impedances, Z_e and Z_o, and the modal effective permittivities, $\varepsilon_{\text{eff}}^e$ and $\varepsilon_{\text{eff}}^o$. Note that this is the same circuit proposed in [11] for a folded hairpin resonator. The symmetry of the structure with respect to the AA' plane in Fig.1 allows us to consider separate even and odd mode excitations [11, 28]. Two

independent resonance conditions are then obtained:

$$\tan\frac{\theta_{\mathrm{s}}}{2}\tan\theta_{\mathrm{o}} = R_{\mathrm{zo}} \quad \text{(odd resonances)} \tag{1}$$

$$\tan\theta_e = -R_{\mathrm{ze}}\tan\frac{\theta_{\mathrm{s}}}{2} \quad \text{(even resonances)} \tag{2}$$

where $R_{\mathrm{zo}} = Z_{\mathrm{o}}/Z_{\mathrm{s}}$, $R_{\mathrm{ze}}Conf = Z_{\mathrm{e}}/Z_{\mathrm{s}}$, θ_{s} is the electrical length of the single line section, and $\theta_{\mathrm{e,o}}$ are the electrical lengths of the even (odd) modes of the coupled lines section. The first resonance frequency, f_0, corresponds to the first odd mode resonance. This is the fundamental frequency determining the operation band of any filter based on these resonators. The first spurious resonance frequency, f_1, corresponds to the first even mode resonance.

2.2. Minimum Size Conditions

The degree of compactness of folded SIR's can be described following the method in [28], where the physical length of the resonator is compared with the length of an open-loop resonator having the same fundamental frequency. This analysis yields the following optimal values for the electrical lengths of the single and coupled line sections
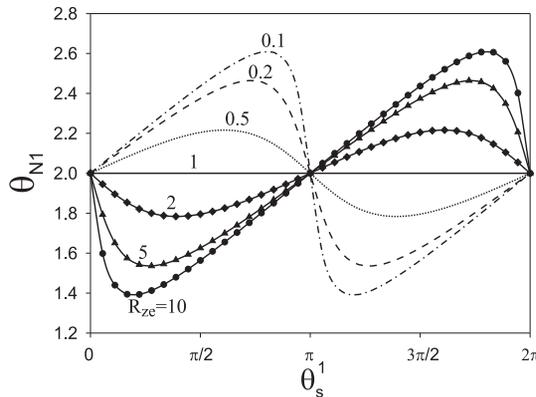
Figure 3. Normalized electrical length at the first spurious resonance frequency (f_1) of SIR's versus θ_{s}^1 using the ratio R_{ze} as a parameter.

($R_{zo} < 1$ is assumed):

$$\theta_{s}^{0} = 2 \tan^{-1} \sqrt{\frac{R_{zo}(R_{zo}P_{s} - P_{o})}{R_{zo}P_{o} - P_{s}}} \tag{3}$$

$$\theta_{o}^{0} = \tan^{-1} \sqrt{\frac{R_{zo}(R_{zo}P_{o} - P_{s})}{R_{zo}P_{s} - P_{o}}} \tag{4}$$

where $P_{s} = \sqrt{\varepsilon_{eff}^{ref}/\varepsilon_{eff}^{s}}$ and $P_{o} = \sqrt{\varepsilon_{eff}^{ref}/\varepsilon_{eff}^{o}}$, ε_{eff}^{ref} being the effective permittivity of the transmission line used to implement the open-loop resonator (note that if $P_{s} = 1$ we recover the results in [29] and if $P_{s} = P_{o} = 1$ we are in the case treated in [30]). In brief, we conclude that, for miniaturization purposes, the SIR must be designed so as to get values of R_{zo}, P_{s} and P_{o} as small as possible whereas θ_{s}^{0} and θ_{o}^{0} fulfill the minimum conditions in (3) and (4).

2.3. Pushing up the First Spurious Resonance

It is our goal to maximize the ratio f_{1}/f_{0}. In other words, the electrical length of the SIR at f_{1} should be as large as possible when compared with the electrical length of our reference half-wave resonator at f_{0} (i.e., π). Let us define the normalized electrical length at the first spurious resonance of a SIR as $\theta_{N1} = (\theta_{s}^{1} + 2\theta_{e}^{1})/\pi$. The electrical lengths θ_{s}^{1} and θ_{e}^{1} are, respectively, the lengths of the single line section and the even mode electrical length of the coupled section of the SIR at f_{1}. In Fig. 3, we plot the values of θ_{N1} as a function of θ_{s}^{1} using the ratio R_{ze} as a parameter. The case $R_{ze} = 1$ corresponds to the half-wave open-loop resonator and, obviously, $\theta_{N1} = 2$ in such case. If $R_{ze} < 1$ θ_{N1} reaches a maximum when $\tan(\theta_{s}^{1}/2) = 1/\sqrt{R_{ze}}$ (in that case $\theta_{e}^{1} = \theta_{s}^{1}/2 + \pi/2$) and a minimum when $\tan(\theta_{s}^{1}/2) = -1/\sqrt{R_{ze}}$ (in that case $\theta_{e}^{1} = \theta_{s}^{1}/2 - \pi/2$). On the contrary, if $R_{ze} > 1$, θ_{N1} reaches a minimum when $\tan(\theta_{s}^{1}/2) = 1/\sqrt{R_{ze}}$ (in that case $\theta_{e}^{1} = \theta_{s}^{1}/2 + \pi/2$) and a maximum when $\tan(\theta_{s}^{1}/2) = -1/\sqrt{R_{zo}}$ (in that case $\theta_{e}^{1} = \theta_{s}^{1}/2 - \pi/2$). This discussion is not completely equivalent to the similar analysis carried out in [28] for folded hairpin resonators because in [28] only the range $\pi < \theta_{s}^{1} < 2\pi$ (or $\theta_{s}^{1}/2 > \theta_{e}^{1}$) was considered. Thus the authors of [28] conclude that, to increase the first spurious frequency, it is necessary that $R_{ze} > 1$. However, the reverse condition, i.e., $R_{ze} < 1$ might also lead to increase the first spurious frequency in the range $0 < \theta_{s}^{1} < \pi$ (or $\theta_{s}^{1}/2 < \theta_{e}^{1}$). An important reference concerning this discussion, but focused on the unfolded version of the conventional SIR, can be found in [31].
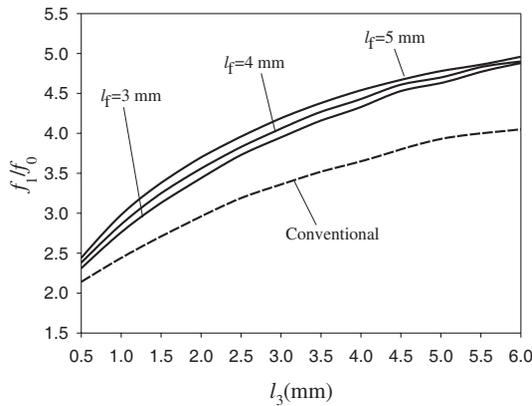
Figure 4. Variation of f_1/f_0 as a function of the length of the coupled lines section (l_3). The dashed line corresponds to a conventional folded SIR. Solid lines correspond to folded SIR with floating conductors having different values of l_f and $s = 0.1$ mm.

In conclusion, the double goal of optimum miniaturization and maximum ratio f_1/f_0 can be reached provided the conditions discussed in this section and (3) and (4) are simultaneously fulfilled. But this is not a trivial task because usually the involved electrical parameters are not independent. For a given substrate, effective dielectric constants and characteristic impedances are strongly interleaved. However, additional flexibility would be obtained if the values of R_{zo} and R_{ze} could be separately controlled. In such case, the designer could independently tune, within a certain range of values, the positions of the fundamental and the first spurious resonance frequencies. This is the advantage provided by the structure proposed in this paper. In the conventional folded SIR the electric field in both the odd and even modes is strongly confined inside the dielectric substrate and Z_e tends to be similar to Z_o. Therefore the miniaturization leads to a lack of control of the first spurious frequency because the value of Z_e can not be tuned independently of Z_o. This is not the case for the modified folded SIR in Fig. 1. For the first (odd) resonance, the floating conducting patch behaves, roughly speaking, as a grounded conductor. The parameters of the coupled lines Z_o and $\varepsilon_{\text{eff}}^{\text{o}}$ are, approximately, the same as those the conventional folded SIR. Therefore, we would not expect an important modification of the fundamental resonance frequency with respect to that of the conventional folded SIR. However, for the first even resonance, the behavior of the floating conductor is far away of being a virtual ground plane. In such case, the electric field

is not confined in the substrate and, even if Z_o is chosen to be very low, a wide range of values of Z_e is achievable tuning the dimensions of the floating conductor. Thus, the designer has a higher level of control on the separation of the two first resonance frequencies. This feature of the the structure in Fig. 1 is exploited in this paper. In Fig. 4, we plot the ratio f_1/f_0 as a function of l_3 for several values of the parameter l_f (SIR with floating conductor) and for the conventional folded SIR. The new structure allows us to obtain values of this ratio larger than the ratio provided by conventional folded SIR.

2.4. Some Practical Examples

In order to check the theoretical considerations above, we have numerically studied the behavior of several electrical parameters of conventional folded SIR's and the modified SIR in this paper. The resonators are supposed to be printed on a commercial substrate of relative dielectric permittivity $\varepsilon_r = 10.2$ and thickness $h = 0.254\,\text{mm}$. This substrate has been used later to obtain experimental results. The printed circuit is enclosed in a metallic box whose dimensions have been taken into account in the calculations. The physical size of the inductive region has been chosen to be the same for all the resonators. Therefore, the dimensions $w_0 = 0.37\,\text{mm}$, $l_1 = 3.075\,\text{mm}$, $l_2 = 1.68\,\text{mm}$ are the same for all of them. We also keep constant the value $l_4 = 3.025\,\text{mm}$. Using the fast solver described in [32] we can compute the required electrical parameters. For the conventional SIR we have $Z_s = 39.72\,\Omega$, $\varepsilon_{\text{eff}}^s = 7.06$, $Z_o = 7.69\,\Omega$, $\varepsilon_{\text{eff}}^o = 8.09$, $Z_e = 8.93\,\Omega$ and $\varepsilon_{\text{eff}}^e = 9.33$. Note that, as predicted, Z_e and Z_o are low, as required for miniaturization, but close to each other, what is not suitable to get high values of f_1/f_0. For the folded SIR with floating conductor $Z_s = 61.85\,\Omega$, $\varepsilon_{\text{eff}}^s = 4.97$. For this structure, the values of Z_o, $\varepsilon_{\text{eff}}^o$, Z_e and $\varepsilon_{\text{eff}}^e$ depend on the dimensions of the floating conductor, s and l_f in Fig. 1. Our computations show that odd mode parameters of the coupled section slightly depend on s but are invariant with respect to l_f. For values of s ranging from $0.1\,\text{mm}$ to $1.0\,\text{mm}$, Z_o varies between 7.7 and $9.2\,\Omega$. These values are similar to the value of Z_o for the conventional folded SIR. Although $\varepsilon_{\text{eff}}^s$ is smaller for the newly proposed resonator, the relatively high value of Z_s compensates this effect and makes f_0 slightly smaller in the case of the SIR with floating conductor. However, it is the effect on f_1 what is more important. The values of Z_e for our resonator quickly increases with the value of l_f and is not difficult to obtain values of this parameter 5 or 6 times higher than the value of $8.93\ \Omega$ corresponding to the conventional folded SIR.
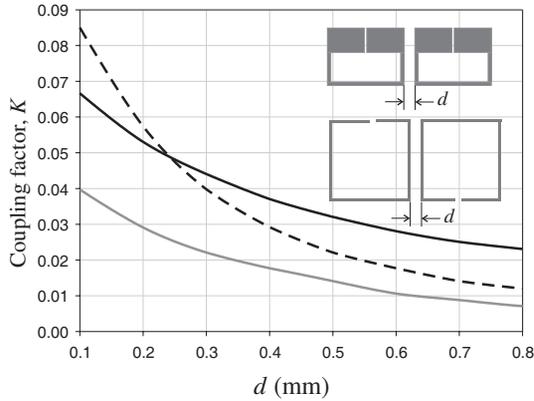
Figure 5. Coupling factor versus the distance between adjacent resonators for the different resonator geometries used to design filter A. Black solid line: folded SIR with floating conductor; grey solid line: conventional folded SIR; black dashed line: open-loop resonator.

## 3. EXAMPLES OF BANDPASS FILTER DESIGNS

Several filters with similar specifications have been designed and fabricated using conventional open-loop, folded SIR resonators, and the newly proposed folded SIR with floating conductor.

3.1. Example 1: Three Poles Filter

Let us consider the following specs for filter A: order $N = 3$, central frequency $f_0 = 900$ MHz, ripple = 0.1 dB and fractional bandwidth = 4%. The same substrate considered in the previous section has been used. The filters were placed inside a metallic enclosure whose dimensions were 40×20 mm^2. The thicknesses of the air layers below and above the substrate were chosen to be 2.0 mm. It is worth mentioning that the effect of the metallic enclosure on the pass band and first spurious band is marginal because the electromagnetic field is highly confined around metallic strips and slots. The response of the filter at those frequencies is governed by the printed metallization and is not meaningfully influenced by the enclosure. Note that this is not the case for other suspended substrate structures [14], where the enclosure dimensions are critical to the design. This is a practical advantage of our proposal since the filter can be integrated as a part of a more complex system without modifications associated to housing. Nevertheless, intentionally designed small housing can be

advantageously used to reduce the transmission levels in the frequency region between desired and spurious bands, as it will be shown later. Of course, the size of the housing should not be too large so as to avoid spurious resonances degrading the rejection level above and near the pass band. Radiation is important only at the spurious band frequency region.

The folded SIR's used in the experiments share the following dimensional parameters: $w_0 = 0.37$ mm, $l_1 = 4.28$ mm, $l_2 = 3.4$ mm and $l_4 = 4.23$ mm. The values of l_3 yielding the resonance at f_0 for each resonator are: $l_3 = 6.0$ mm (conventional folded SIR) and $l_3 = 4.2$ mm (folded SIR with floating conductor). For the floating conductor $w_f = 3.8$ mm, $l_f = 7.85$ mm, $s = 0.35$ mm and $w_f = 3.8$ mm. For comparison purposes we have added a design based on the open-loop resonator: the strip width is also 0.37 mm and the microstrip length to fit f_0 is 64.4 mm. We have followed the standard design procedure based on the determination of the coupling factor between adjacent resonators [33, Chap. 8]. The coupling factor is depicted in Fig. 5 as a function of the separation, d, between resonators. In this figure, an interesting additional feature of the resonator proposed in this paper can be appreciated: the coupling factor is larger than of the conventional folded SIR or the open-loop resonator except for very small separations. This means that, for a given bandwidth, the proposed geometry is less sensitive to dimensional tolerances and, conversely, that larger bandwidths can be achieved. The specs of filter A lead to a coupling factor of $K = 0.037$. This requires extremely close conventional folded SIR's. However, the gap between the resonators with floating rectangular patch is relatively large and of easy fabrication. The external quality factor for the in-out resonators
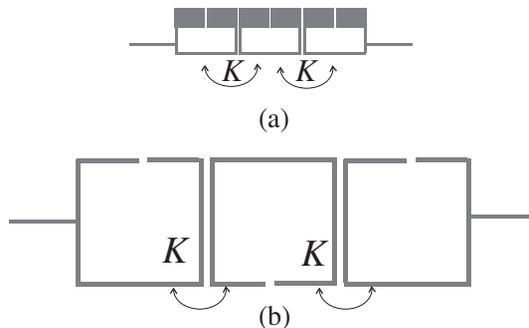

Figure 6. Layouts of the third-order filters based on folded SIR's and open loop resonators. The electrical responses are in Fig. 7.

(a)

(b)
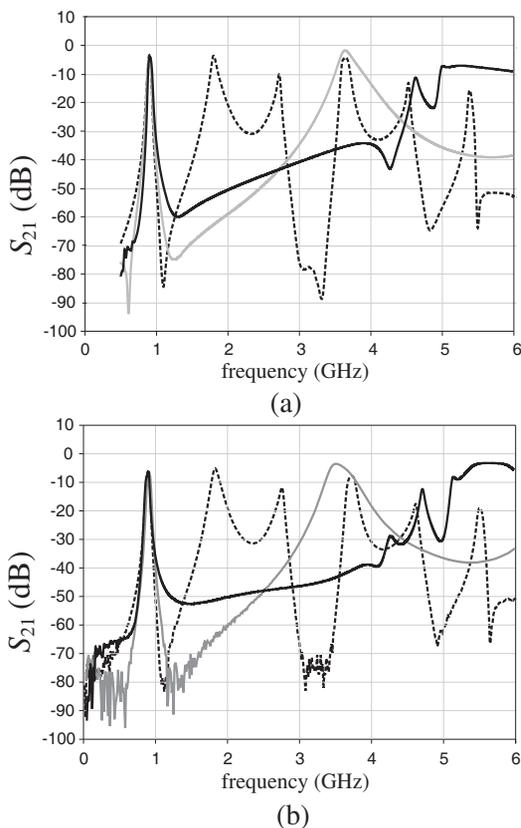
Figure 7. (a) Simulated and (b) measured broadband insertion losses of the three fabricated filters with the specs of filter A. Black solid line: filter based on folded SIR with floating conductor (area: 201 mm^2); grey solid line: filter based on conventional folded SIR (area: 243 mm^2); black dashed line: filter based on open-loop resonator (area: 813 mm^2).

turns out to be $Q = 25.8$. In Fig. 6, we show the layouts of the folded SIR based and open loop based filters. Simulated and measured broadband insertion losses of the three filters fabricated with the above mentioned resonators are plotted in Fig. 7. As a first advantage, the filter based on the resonator with floating conductor provides the desired pass band with less stringent conditions for gap dimensions. Moreover, the rejection level in the upper rejection band is much better for the filter based on this resonator. And last but not least, the filter based on the new resonator is the smallest one: 20% area reduction

with respect to conventional folded SIR implementation. Note that the folded resonators used in our filters are truly quasi-lumped. Indeed, the overall length is below $\lambda_0/12$, λ_0 being the free space wavelength at f_0. A simple lumped element quasi-static model could be then used. This was not the case for the folded SIR's used in [14], for instance. This means that, although the upper rejection band reported in [14] is as good as the one obtained in this paper, the filter in [14] is not electrically small.
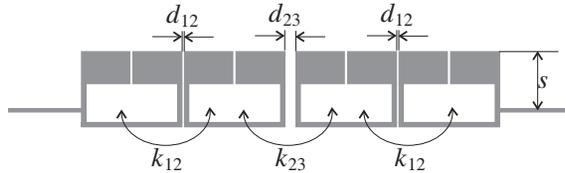

Figure 8. Layout of a fourth-order filter based on the resonators proposed in this paper. Floating conductors (not shown) are printed on the backside of the substrate. The electrical response of the filter is in Fig. 9.

3.2. Example 2: Four Poles Filter

Let us now consider the design of a filter based on the proposed resonator having a larger relative bandwidth. The specifications of filter B are: order $N = 4$, central frequency $f_0 = 1.43$ GHz, ripple $= 0.1$ dB and fractional bandwidth $= 6\%$. The substrate is the same used in the previous designs. The resonator geometry values are: $l_1 = 3.08$ mm, $l_2 = 1.68$ mm, $l_3 = 3.91$ mm, $l_4 = 3.03$ mm, $l_f = 5.55$ mm, $s = 0.47$ mm and $w_f = 3.3$ mm. The coupling factors associated to the filter specs are $K_{12} = 0.045$ and $K_{23} = 0.039$. The layout of the filter is drawn in Fig. 8. These values lead to gap dimensions $d_{12} = 0.1$ mm and $d_{23} = 0.25$ mm. If we try to fabricate the same filter with the conventional folded SIR, the smallest gap required between resonators is less than 30 microns. This is well below of the limit of our fabrication process and dimensional tolerances would become critical even with more accurate fabrication techniques. The external quality factor for the in-out resonators is $Q = 18.5$. To achieve this value, the position of the 50 Ω ($w = 0.24$ mm) feed lines along one of the sides of the input and output resonators is given by $s = 4.31$ mm. Fig. 9 shows the response of the filter in and around the passband. The -30 dB level in the insertion loss curve is reached at about 5.3 GHz. The patterned substrate was placed inside the metallic box shown in Fig. 10.
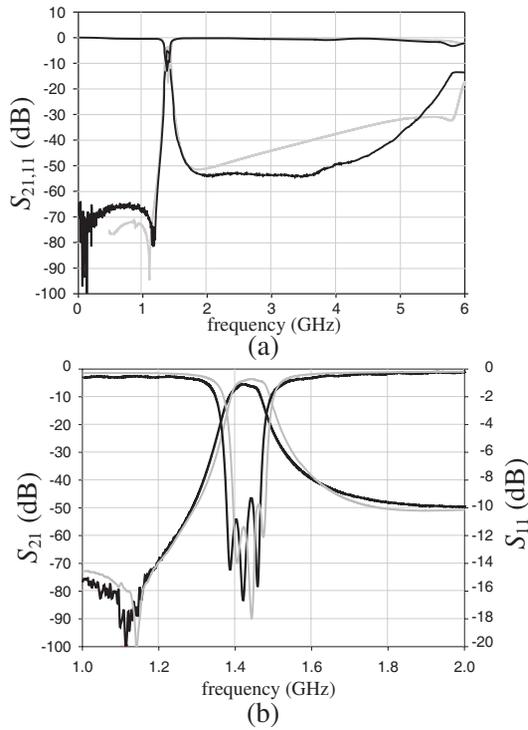
Figure 9. Simulated (grey solid line) and measured (black solid line) response of filter B around the passband region. The filter has been fabricated using the folded stepped impedance resonator including floating conductor proposed in this paper.
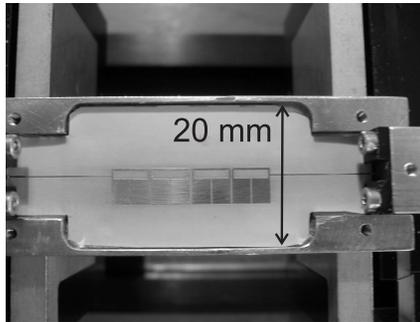
Figure 10. A photograph of the filter B with the top lid removed.
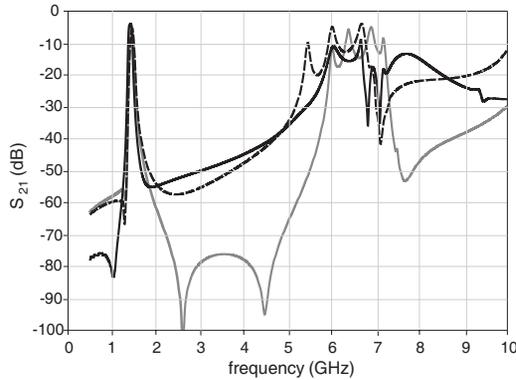
Figure 11. Wide band computed response of the filter B: a) The solid black line corresponds to Ensemble simulation without consideration of the finite width of the box; b) The dotted line corresponds to HFSS simulation for a relatively large box width: 16.00 mm; c) the solid grey line corresponds to HFSS simulation for a relatively small box width: 8.0 mm.

It has been mentioned that, if the box dimensions were allowed to be freely chosen, very good rejection levels could be reached in the frequency band above the first pass band. Full-wave simulations of the filter B using HFSS have been carried out for two different box widths and the results are shown in Fig. 11. Ensemble simulation for infinitely wide box is included for comparison purposes. Note that for a box width of 16 mm Ensemble and HFSS results are very close to each other. However, a box width of 8 mm gives place to very small transmission levels in between the desired and spurious pass bands. The reason is that, in the 8 mm width case, the quasi TE_{10} mode supported by the enclosure is far away from cutoff. The very strong reactive attenuation of the fields associated to this mode precludes significant transmission. Note that almost 80 dBs attenuation are reached. However, for a 16 mm wide box, the evanescent electromagnetic field is still large enough at the output port so as to limit attenuation levels to 40–50 dBs. The pass bands are only slightly affected by the proximity of the lateral walls, but the rejection level in the middle of the pass bands strongly depends on the details of the waveguide modes of the box. Finally we should comment on the transmission zeros observed at measurements and simulations that are not accounted for by the equivalent circuit of the filter. These zeros are due to destructive interference between the waves supported by the microstrip system and the waves associated to other weak transmission mechanisms: substrate surface waves, evanescent fields of the box, and

so on. These mechanisms are not included in the circuit model. This interference is only meaningful at those frequencies where the circuit model predicts low transmission levels.

4. CONCLUSIONS

In this paper we have modified the conventional folded SIR used in the fabrication of passband filters by including a ground plane window with a floating conductor. A detailed analysis of the new resonator based on a transmission line circuit model has been carried out. In particular, we have demonstrated the possibility of separately controlling the fundamental and the first spurious resonances of the SIR with ground plane aperture and floating conductor. This allows us to improve the rejection level in the upper rejection band when compared with filters based on conventional folded SIR's. Size reduction and higher coupling level between resonators – with the possibility of increased bandwidth – have also been demonstrated. Several filter designs have been included to show the potential of the new resonant structure. The use of a suitably designed enclosure gives place to excellent rejection level in the out of band region.

ACKNOWLEDGMENT

REFERENCES

1. Nedil, M., T. A. Denidni, A. Djaiz, and H. Boutayeb, "ULtra-wideband bandpass filters using multilayer slot coupled transitions," *Journal of Electromagnetic Waves and Applications*, Vol. 22, No. 4, 501–516, 2008.

2. Zhang, X.-C., J. Xu, and Z.-Y. Yu, "Design of quasi-elliptic bandpass filter based on slow-wave open-loop resonators," *Journal of Electromagnetic Waves and Applications*, Vol. 22, 1849–1856, 2008.

3. Razalli, M. S., A. Ismail, M. A. Mahdi, and M. N. Hamidon, "Novel compact "via-less" ultra wideband filter utilizing capacitive microstrip patch," *Progress In Electromagnetics Research*, Vol. 88, 91–104, 2008.

4. AlHawari, A. R. H., A. Ismail, M. F. A. Rasid, R. S. A. R. Abdullah, B. K. Esfeh, and H. Adam, "Compact microstrip bandpass filter with sharp passband skirts using square spiral resonators and embedded resonators," *Journal of Electromagnetic Waves and Applications*, Vol. 23, 675–683, 2009.

5. Yu, W.-H., J.-C. Mou, X. Li, and X. Lv, "A compact filter with sharp transition and wideband rejection using the novel defected ground structure," *Journal of Electromagnetic Waves and Applications*, Vol. 23, 329–340, 2009.

6. Razalli, M. S., A. Ismail, M. A. Mahdi, and M. N. Hamidon, "Novel compact "via-less" ultra wideband filter utilizing capacitive microstrip patch," *Progress In Electromagnetics Research*, Vol. 91, 213–227, 2009.

7. Tao, Y., M. Tamura, and T. Itoh, "Compact hybrid resonator with series and shunt resonances used in miniaturized filters and balun filters," *IEEE Trans. on Microwave Theory and Tech.*, Vol. 58, 390–402, 2010.

8. Cohn, S. B., "Parallel-coupled transmission-line resonator filters," *IRE Trans. on Microwave Theory and Tech.*, Vol. 6, 223–231, 1958.

9. Crystal, E. G. and S. Frankel, "Hairpin-line and hybrid hairpin-line/half-wave parallel-coupled-line filters," *IEEE Trans. on Microwave Theory and Tech.*, Vol. 20, 719–728, 1972.

10. Hong, J. S. and M. J. Lancaster, "Couplings of microstrip square open loop resonators for cross-coupled planar microwave filters," *IEEE Trans. on Microwave Theory and Tech.*, Vol. 44, 2099–2018, 1996.

11. Sagawa, M., K. Takahashi, and M. Makimoto, "Miniaturized hairpin resonator filters and their application to receiver front-end MIC's," *IEEE Trans. on Microwave Theory and Tech.*, Vol. 37, 1991–1997, 1989.

12. Hong, J. S. and M. J. Lancaster, "Theory and experiment of novel microstrip slow-wave open-loop resonator filters," *IEEE Trans. on Microwave Theory and Tech.*, Vol. 45, 2358–2365, 1997.

13. Gu, J., F. Zhang, C. Wang, Z. Zhang, M. Qi, and X. Sun, "Miniaturization and harmonic suppression open-loop resonator bandpass filter with capacitive terminations," *IEEE Intnal. Microwave Symposium*, San Francisco (CA, USA), 373–376, 2006.

14. Packiaraj, D., M. Ramesh, and A. T. Kalghatgi, "Design of a tri-section folded SIR filter," *IEEE Microwave and Wireless Comp. Lett.*, Vol. 16, 317–319, 2006.

15. Akkaraekthalin, P. and J. Jantree, "Microstrip slow-wave open-loop slow resonator filters with reduced size and improvedIn conclusion stopband characteristics" *ETRI Journal*, Vol. 28, 607–614, 2006.

16. Wang, Y. X., "Microstrip cross-coupled tri-section stepped-impedance bandpass filter with wide stop-band performance," *Journal of Electromagnetic Waves and Applications*, Vol. 23, 289–296, 2009.

17. Wang, J. P., B. Z. Wang, Y. X. Wang, and Y. X. Guo, "Dual-band miceostrip stepped-impedance bandpass filter with defected ground structure," *Journal of Electromagnetic Waves and Applications*, Vol. 22, No. 4, 463–470, 2008.

18. Sheta, A. F., "A novel compact degenerate dual-mode square patch filter using cross H-shaped defected ground structure," *Journal of Electromagnetic Waves and Applications*, Vol. 22, 1913–1923, 2008.

19. Guo, Y. C., L. H. Weng, and X. W. Shi, "An improved microstrip open-loop resonator bandpass filter with DGSS for WLAN applications," *Journal of Electromagnetic Waves and Applications*, Vol. 23, 463–472, 2009.

20. Packiaraj, D., K. J. Vinoy, and A. T. Kalghatgi, "Analysis and design of two layered ultra wide band filter," *Journal of Electromagnetic Waves and Applications*, Vol. 23, 1235–1243, 2009.

21. Quendo, C., E. Rius, C. Person, and M. Ney, "Integration of optimized low-pass filters in a bandpass filter for out-of-band improvement," *IEEE Trans. on Microwave Theory and Tech.*, Vol. 49, 2376–2383, 2001.

22. Sun, S. and L. Zhu, "Stopband-enhanced and size-miniaturized low-pass filters using high-impedance property of offset finite-ground microstrip line," *IEEE Trans. on Microwave Theory and Tech.*, Vol. 53, 2844–2850, 2005.

23. Velázquez-Ahumada, M. C., J. Martel, and F. Medina, "Design of compact low-pass elliptic filters using double-side MIC technology," *IEEE Trans. on Microwave Theory and Tech.*, Vol. 55, 121–127, 2007.

24. Zhang, W., L. Han, R. Ma, and J. Mao, "Multiharmonic supression band-pass filter for communication system," *ETRI Journal*, Vol. 29, 533–535, 2007.

25. García, J., J. Bonache, I. Gil, F. Martín, M. C. Velázquez, and J. Martel, "Miniaturized microstrip and CPW filters using coupled metamaterial resonators," *IEEE Trans. on Microwave Theory and*

Tech., Vol. 54, 2628–2635, 2006.

26. Masot, F., F. Medina, and M. Horno, "Analysis and experimental validation of a type of three-microstrip directional coupler," *IEEE Trans. on Microwave Theory and Tech.*, Vol. 42, 1624–1631, 1994.

27. Velázquez-Ahumada, M. C., J. Martel, and F. Medina, "Parallel coupled microstrip filters with floating ground-plane conductor for spurious-band suppression," *IEEE Trans. on Microwave Theory and Tech.*, Vol. 53, 1823–1828, 2005.

28. Lee, S. Y. and C. M. Tsai, "New cross-coupled filter design using improved hairpin resonator," *IEEE Trans. on Microwave Theory and Tech.*, Vol. 48, 2482–2490, 2000.

29. Zhu, J. and Z. Feng, "Microstrip interdigital hairpin resonator with an optimal physical length," *IEEE Microwave and Wireless Comp. Letters*, Vol. 16, 672–674, 2006.

30. Makimoto, M. and S. Yamashita, *Microwave Resonators and Filters for Wireless Communication*, Springer Series in Advanced Electromagnetics, New York, 2001.

31. Lee, S.-Y., "Optimum resonant conditions of stepped impedance resonators," *European Microwave Conference*, 2005.

32. Martel, J. and F. Medina, "A suitable integral equation for the quasi-TEM analysis of hybrid strip/slot-like structures," *IEEE Trans. on Microwave Theory and Tech.*, Vol. 49, 224–228, 2001.

33. Hong, J. S. and M. J. Lancaster, *Microstrip Filters for RF/Microwave Applications*, New York, Wiley, 2001.